A Matrix Isolation Spectroscopic and Quantum Chemical Study of Fumaric and Maleic Acid

Ermelinda M. S. Maçôas,[†] **Rui Fausto,**[*,†] **Jan Lundell,**[‡] **Mika Pettersson,**[‡]
Leonid Khriachtchev,[‡] **and Markku Räsänen**[‡]

Department of Chemistry - CQC, University of Coimbra, P-3049 Coimbra, Portugal, and Laboratory of Physical Chemistry, University of Helsinki, P.O. Box 55 (A.I. Virtasen aukio 1), FIN-00014 Helsinki, Finland

Received: October 16, 2000; In Final Form: January 29, 2001

Relative energies and vibrational spectra of buthenedioic acid [(*E*)- and (*Z*)-HOOC−CH═CH−COOH; fumaric and maleic acids] were calculated using Hartree−Fock (HF), Møller−Plesset to 2nd order (MP2), and B3LYP Density Functional Theory (DFT) levels of approximation. Computationally the lowest energy conformer of maleic acid has a nearly planar structure with an OH···O═C intramolecular hydrogen bond closing a seven member O═C−C(H)═C(H)-C−O−H ring. Second conformer of maleic acid adopts a cis arrangement around the C−O bonds and exhibits the two carbonyl bonds in a nearly orthogonal arrangement with one carboxylic group in the plane containing the carbon atoms. Fumaric acid has three planar conformers with relative energies within 5 kJ mol⁻¹. These conformers exhibit a cis arrangement around the C−O bond and differ by the relative conformation of their O═C−C═C axes. The infrared spectra of the studied compounds isolated in a solid argon matrix feature the most stable conformers. Narrowband tunable irradiation in the near-infrared region (6901 cm⁻¹) was found to promote a conversion of the second most stable conformer of maleic acid into the most stable conformer.

Introduction

Both (*E*)- and (*Z*)-buthenedioic acids (fumaric and maleic acids) have important practical applications in polymer industry[1−4] and in medicine, in particular as anti-fungicides and antitumoral agents.[5−9] In a more fundamental perspective, studies on their structural and spectroscopic properties is important, since they are the simplest dicarboxylic acids exhibiting a carbon−carbon double bond. Despite the wide range of application of these carboxylic acids, to the best of our knowledge, there are no studies on monomeric fumaric and maleic acids available, the existing information concerning essentially with the structure of their crystalline phases.[10−12]

Detailed structural and vibrational studies were reported for the monocarboxylic parent molecule, propenoic acid (acrylic acid, CH₂═CHCOOH),[13] and the related molecules, (*Z*)- and (*E*)-3-methyl-propenoic [(*Z*)- and (*E*)-crotonic acid, CH₃CH═CHCOOH].[14,15] These studies revealed that these molecules exist both in the gas phase and in solid argon in two conformational states differing by internal rotation around the C_α−C bond and having similar energies [$\Delta E_{(s-trans)-(s-cis)} \approx 3$ kJ mol⁻¹]. The s-cis conformer (C═C_α−C═O dihedral equals to 0°) was found to be the conformational ground state for the three molecules.[13−15] Ultraviolet irradiation ($\lambda_{exc} = 243$ nm) of matrix isolated (*E*)-crotonic acid was found to promote conformational isomerization from the s-cis conformer to the s-trans conformer (C═C_α−C═O dihedral equals to 180°) as well as conversion to (*Z*)-crotonic acid, the latter process being noticeably more efficient than the first one.[14,15]

In this article, we present a detailed study of the conformers of monomeric maleic and fumaric acids combining ab initio and Density Functional Theory (DFT) calculations and matrix isolation vibrational spectroscopy with selective near-infrared induced rotamerization. In particular, the main factors which determine the stability of different conformers, their vibrational signature and the photoinduced interconversion processes between the lowest energy species are analyzed.

Experimental and Computational Details

The matrix samples were prepared by continuously flushing a copper tube containing maleic or fumaric acid (Aldrich, 99+%), heated to 353 and 408 K, respectively, with high purity argon (Aga, 99.9999%). The gaseous mixtures were deposited onto a cooled CsI window in a close-cycle helium cryostat (APD, DE202A) at 7.5 K. In our samples, monomeric species were almost exclusively formed, which was achieved by choosing an appropriate temperature of the substance container and optimizing the matrix gas flow rate. The IR spectra (4000−400 cm⁻¹) were measured with a Nicolet SX-60 FTIR spectrometer equipped with a liquid nitrogen cooled MCT detector and a KBr beam splitter, with spectral resolutions of 0.25 or 1.0 cm⁻¹. Typically 200 interferograms were coadded.

Photoexcitation was performed using a tunable pulsed near-infrared (NIR) radiation provided by an optical parametric oscillator (OPO Sunlite, Continuum) pumped by an Nd:YAG solid-state laser (Powerlite 9010, Continuum). The pulse duration of the NIR irradiation was ca.5 ns with a line width of ∼0.1 cm⁻¹. The NIR radiation wavenumber was established with an accuracy better than 1 cm⁻¹ by a Burleigh WA-4500 wavemeter used to control the OPO signal radiation wavelength. Broadband IR irradiation and UV excitation of fumaric acid were under-taken using the globar of the spectrometer and the Nd:YAG laser ($\lambda = 266$ nm), respectively.

The ab initio and DFT calculations[16−18] were performed with

Study of Fumaricand Maleic Acid

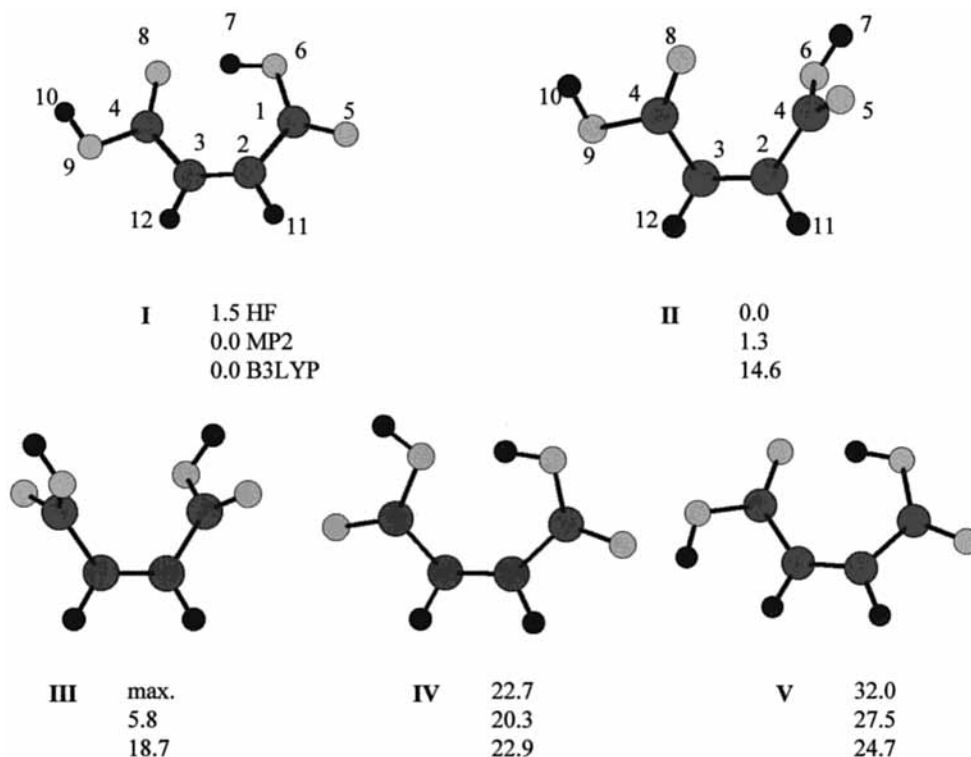*J. Phys. Chem. A, Vol. 105, No. 15, 2001* **3923**

Figure 1. Structure and relative energies (kJ mol^{-1}) of most stable conformers of maleic acid predicted at three different theoretical levels. The relative energies account for the zero-point-vibrational-energy correction.

Figure 2. Structure and relative energies (kJ mol^{-1}) of the most stable conformers of fumaric acid predicted at three different theoretical levels. The relative energies account for the zero-point-vibrational-energy correction.
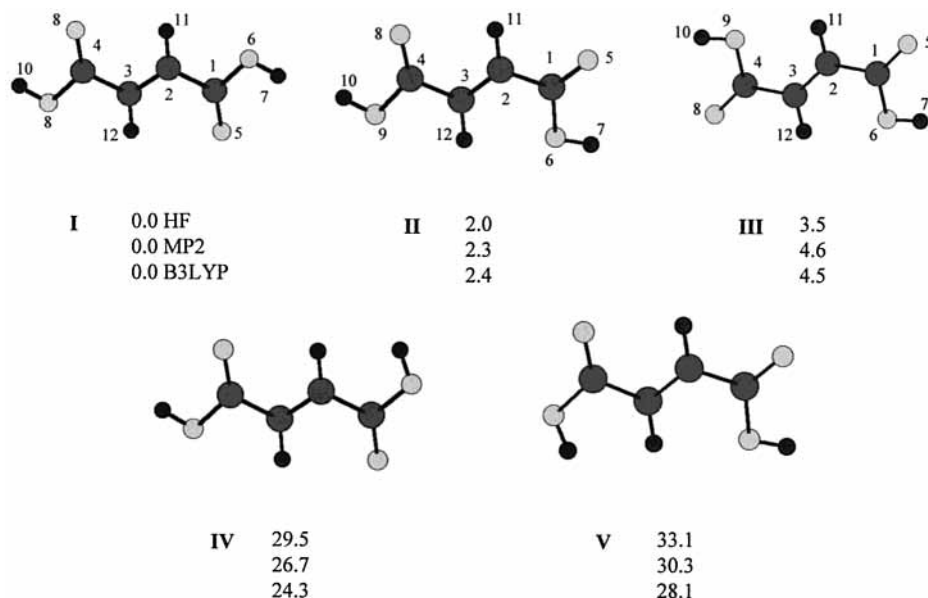
GAUSSIAN 92/DFT or 94[19] on a DEC ALPHA 7000 computer at the Center of Informatics of the University of Coimbra and on a SGI Origin 2000 at the CSC−Center for Scientific Computing, Ltd. (Espoo, Finland). Geometry optimizations were performed at three different levels of theory [Hartree−Fock (HF), Møller−Plesset to 2nd order (MP2), and B3LYP Density Functional Theory (DFT)] using the 6-31G(d,p) basis set.[20,21] Vibrational calculations were performed to ensure that the found stationary points were true minima and not transition states. We report here only the B3LYP/6-31G(d,p) frequencies in consonance with our previous work on malonic acid.[22] The force constants (symmetry internal coordinates) to be used in the normal coordinate analysis were obtained from the DFT

Cartesian harmonic force constants using the program TRANS-FORMER.[23] This program was also used to prepare the input data for the normal coordinate analysis programs used in this study (BUILD-G, and VIBRAT).[24]

Results and Discussion

Molecular Geometries and Energetics. To find the most stable conformations of maleic and fumaric acids we performed a systematic search on their HF/6-31G(d) potential energy surfaces (PES). These calculations are relatively inexpensive in computational terms and yield reasonable structural data for similar compounds.[25] The HF/6-31G(d) calculations were then

TABLE 1: MP2 and B3LYP Geometrical Parameters of Maleic Acid Conformers Obtained Using the 6-31G(d,p) Basis Set

geometrical parameters	conformer			
	MP2		B3LYP	
	I	II	I	II
bond (pm)				
$C_1=O_5$	122.2	121.7	121.5	121.0
C_1-O_6	133.7	135.2	133.0	134.6
O_6-H_7[a]	98.3	97.2	99.0	97.3
C_2-C_1	150.5	149.6	151.1	150.0
C_2-H_{11}	108.2	108.3	108.6	108.7
$C_2=C_3$	135.0	134.1	134.6	133.7
C_3-H_{12}	108.2	108.1	108.6	108.5
C_3-C_4	147.6	148.0	147.6	148.3
$C_4=O_8$[a]	123.1	122.1	122.6	121.4
C_4-O_9	134.6	135.7	134.3	135.5
O_9-H_{10}	97.2	97.1	97.3	97.2
$C_4=O_8 \cdots H_7-O_6$	168.0		164.7	
angle (deg)				
$C_2-C_1=O_5$	117.6	123.7	117.4	122.8
$O_5=C_1-O_6$	121.8	124.4	122.1	124.2
$C_1-O_6-H_7$	111.4	105.6	112.0	106.3
$C_1-C_2=C_3$	133.9	124.5	133.8	126.2
$C_1-C_2-H_{11}$	109.9	115.5	109.5	114.2
$C_4-C_3=C_2$	128.2	121.6	127.9	122.8
$C_4-C_3-H_{12}$	114.0	117.5	113.8	116.7
$C_3-C_4=O_8$	127.6	125.7	127.3	126.0
$O_8=C_4-O_9$	121.8	123.4	121.3	122.9
$C_4-O_9-H_{10}$	106.4	105.7	107.0	106.2
dihedral angle (deg)				
$O_5=C_1-O_6-H_7$	180.0	−5.5	180.0	−5.5
$O_5=C_1-C_2-C_3$	180.0	105.9	180.0	109.8
$C_1-C_2-C_3-C_4$	0.0	1.1	0.0	1.2
$O_8=C_4-O_9-H_{10}$	0.0	0.1	0.0	0.1
$O_8=C_4-C_3-C_2$	0.0	−8.6	0.0	−7.4
$H_{11}-C_2-C_3-H_{12}$	0.0	1.6	0.0	−1.8

[a] $C_4=O_8$ and O_6-H_7 bond lengths in conformer I clearly show the intermolecular $O_6-H_7 \cdots O_4=C_8$ hydrogen bond in this conformer as they are clearly longer than in the free O−H and C=O bonds in conformer II.

used as the first estimate to the MP2 and DFT calculations. In these preliminary calculations, the O=C−C=C dihedral angles of the initial structures submitted to geometry optimization were varied by 60° within the range 0−360° and the initial O=C−O−H dihedral angles were made equal to 0° or 180° (all nonequivalent-by-symmetry combinations of the dihedral angles were considered).

Maleic Acid. Following the indications provided by the preliminary HF/6-31G(d) calculations, five conformers of maleic acid are found at the MP2 and B3LYP levels. These conformers are shown in Figure 1, where their relative energies are also given [complete structural results obtained at the HF/6-31G(d) level of theory and MP2 and B3LYP geometries for the highest energy conformers can be received from the authors upon request]. Table 1 shows the MP2 and B3LYP calculated geometries for the two lowest energy conformers. The most stable conformer (I) is nearly planar, with an OH···O=C intramolecular hydrogen bond closing the seven member O=C−C(H)=C(H)−C−O−H ring. The second most stable conformer (II) is nonplanar with cis arrangements around the C−O bonds. The two carbonyl bonds of this conformer are nearly orthogonal with one carboxylic group in the plane containing the carbon atoms.

The energy difference between conformer II and the conformational ground state is estimated to be 14.6 kJ mol^{-1} at the B3LYP level, whereas the MP2 calculations give a considerably smaller difference (1.3 kJ mol^{-1}). As shown later, the MP2 result

TABLE 2: MP2 and B3LYP Geometrical Parameters of Fumaric Acid Conformers Obtained Using the 6-31G(d,p) Basis Set

geometrical parameters	conformers					
	MP2			B3LYP		
	I	II	III	I	II	III
bond (pm)						
$C_1=O_5$	122.0	122.1	122.1	121.4	121.3	121.4
C_1-O_6	135.7	136.0	135.9	135.3	135.5	135.4
O_6-H_7	97.2	97.1	97.1	97.2	97.2	97.2
C_2-C_1	148.2	147.8	147.9	148.5	148.2	148.3
C_2-H_{11}	108.1	108.2	108.0	108.5	108.5	108.4
C_2-C_3	134.2	134.2	134.3	133.7	133.8	133.9
C_3-H_{12}	108.1	108.0	108.0	108.5	108.4	108.4
C_3-C_4	148.2	148.2	147.9	148.5	148.6	148.3
$C_4=O_8$	122.0	122.0	122.1	121.4	121.3	121.4
C_4-O_9	135.7	135.7	135.9	135.3	135.4	135.4
O_9-H_{10}	97.2	97.2	97.1	97.2	97.2	97.2
angle (deg)						
$C_2-C_1=O_5$	125.7	123.9	123.8	125.6	123.6	123.4
$O_5=C_1-O_6$	123.5	123.2	123.2	123.2	123.0	123.0
$C_1-O_6-H_7$	105.9	105.4	105.4	106.3	106.0	106.1
$C_1-C_2=C_3$	120.1	123.7	123.3	120.6	124.3	124.0
$C_1-C_2-H_{11}$	119.0	115.8	115.1	118.5	115.2	114.4
$C_4-C_3=C_2$	120.1	119.6	123.3	120.6	120.2	124.0
$C_4-C_3-H_{12}$	119.0	118.4	115.1	118.5	117.9	114.1
$C_3-C_4=O_8$	125.7	125.8	123.8	125.6	125.7	123.4
$O_8=C_4-O_9$	123.5	123.5	123.2	123.2	123.2	123.0
$C_4-O_9-H_{10}$	105.9	105.8	105.4	106.3	106.3	106.1
dihedral angle (deg)						
$O_5=C_1-O_6-H_7$	0.0	0.0	0.0	0.0	0.0	0.0
$O_5=C_1-C_2-C_3$	0.0	180.0	180.0	0.0	180.0	180.0
$C_1-C_2-C_3-C_4$	180.0	180.0	180.0	180.0	180.0	180.0
$O_8=C_4-O_9-H_{10}$	0.0	0.0	0.0	0.0	0.0	0.0
$O_8=C_4-C_3-C_2$	0.0	0.0	180.0	0.0	0.0	180.0
$H_{11}-C_2=C_3-H_{12}$	180.0	180.0	180.0	180.0	180.0	180.0

agrees much better with the experimentally determined conformer energy difference (1.7 kJ mol^{-1}). These computational results follow the trends previously observed for other dicarboxylic acids where intramolecular hydrogen bonding is important, e.g., 1,3-propanedioic acid.[22] At least for this kind of molecules, the B3LYP calculations tend to overestimate the stabilization energy due to difficulties in describing the intramolecular hydrogen bonding properly. Noteworthy, the HF calculations failed to reproduce the correct energy order of conformers I and II, predicting conformer II as the most stable form ($\Delta E = -1.5$ kJ mol^{-1}). This result is a direct consequence of the inappropriate description of the intramolecular hydrogen bond present in conformer I, and it reinforces our previous conclusions concerning the importance of using higher theoretical levels.[22,25,26] The relative importance of the intramolecular hydrogen bond, as shown by the three theoretical approaches used here, is also clearly evidenced by the calculated values for the OH···O=C distance, which decrease from HF (174.4 pm) to MP2 (168.0 pm) and B3LYP (164.7 pm).

Conformers III−V are predicted by the MP2 calculations to have considerably higher energies than the two most stable forms. This is mostly due to (i) more important repulsive interactions between the lone electron pairs of the carboxylic oxygen atoms and reduced π-delocalization (as in conformer III), (ii) repulsions between hydrogen atoms (as in conformer V, where the $OH_{10} \cdots H_{12}$ repulsion is prevalent), and (iii) presence of trans arrangements around the C−O bonds[27] which are not energetically compensated by strong intramolecular hydrogen bonding (as in conformers IV and V).

Fumaric Acid. For fumaric acid, OH···O=C intramolecular hydrogen bonding involving the two carboxylic groups is not possible and the three computational approaches used (HF, MP2,

TABLE 3: Definition of the Internal Symmetry Coordinates Used in the normal Coordinate Analysis of Maleic and Fumaric Acids

coordinate	symmetry[a]	approximate description[d] C_{2h}[b]	approximate description[d] C_s/C_1[c]	definition[e] C_{2h}[b]	definition[e] C_s/C_1[c]
S1	B_u	ν C=O a.	ν C=O	$(\nu\ C_1{=}O_5) - (\nu\ C_4{=}O_8)$	$\nu\ C_1{=}O_5$
S2	A_g	ν C=O	ν C=O′	$(\nu\ C_1{=}O_5) + (\nu\ C_4{=}O_8)$	$\nu\ C_4{=}O_8$
S3	B_u	ν C−O a.	ν C−O	$(\nu\ C_1{-}O_6) - (\nu\ C_4{-}O_9)$	$\nu\ C_1{-}O_6$
S4	A_g	ν C−O	ν C−O′	$(\nu\ C_1{-}O_6) + (\nu\ C_4{-}O_9)$	$\nu\ C_4{-}O_9$
S5	B_u	ν O−H a.	ν O−H	$(\nu\ O_6{-}H_7) - (\nu\ O_9{-}H_{10})$	$\nu\ O_6{-}H_7$
S6	A_g	ν O−H	ν O−H′	$(\nu\ O_6{-}H_7) + (\nu\ O_9{-}H_{10})$	$\nu\ O_9{-}H_{10}$
S7	B_u	ν C−C a.	ν C−C	$(\nu\ C_1{-}C_2) - (\nu\ C_3{-}C_4)$	$\nu\ C_1{-}C_2$
S8	A_g	ν C−C	ν C−C′	$(\nu\ C_1{-}C_2) + (\nu\ C_3{-}C_4)$	$\nu\ C_3{-}C_4$
S9	B_u	ν C−H a.	ν C−H	$(\nu\ C_2{-}H_{12}) - (\nu\ C_3{-}H_{11})$	$\nu\ C_2{-}H_{12}$
S10	A_g	ν C−H	ν C−H′	$(\nu\ C_2{-}H_{12}) - (\nu\ C_3{-}H_{11})$	$\nu\ C_3{-}H_{11}$
S11	A_g	ν C=C	ν C=C	$\nu\ C_2{=}C_3$	$\nu\ C_2{=}C_3$
S12	B_u	δ COH a.	δ COH	$(\delta\ C_1O_6H_7) - (\delta\ C_4O_9H_{10})$	$\delta\ C_1O_6H_7$
S13	A_g	δ COH	δ COH′	$(\delta\ C_1O_6H_7) + (\delta\ C_4O_9H_{10})$	$\delta\ C_4O_9H_{10}$
S14	B_u	δ OCO a.	δ OCO	$2(\delta\ O_5C_1O_6) - (\delta\ O_5C_1C_2) - (\delta\ O_6C_1C_2) - 2(\delta\ O_8C_4O_9) + (\delta\ O_8C_4C_3) + (\delta\ O_9C_4C_3)$	$2(\delta\ O_5C_1O_6) - (\delta\ O_5C_1C_2) - (\delta\ O_6C_1C_2)$
S15	A_g		δ OCO	δ OCO′	$2(\delta\ O_5C_1O_6) - (\delta\ O_5C_1C_2) - (\delta\ O_6C_1C_2) + 2(\delta\ O_8C_4O_9) - (\delta\ O_8C_4C_3) - (\delta\ O_9C_4C_3)$	$2(\delta\ O_8C_4O_9) - (\delta\ O_8C_4C_3) - (\delta\ O_9C_4C_3)$
S16	B_u	δ CC=O a.	δ CC=O	$(\delta\ O_5C_1C_2) - (\delta\ O_6C_1C_2) - (\delta\ O_8C_4C_3) + (\delta\ O_9C_4C_3)$	$(\delta\ O_5C_1C_2) - (\delta\ O_6C_1C_2)$
S17	A_g	δ CC=O	δ CC=O′	$(\delta\ O_5C_1C_2) - (\delta\ O_6C_1C_2) + (\delta\ O_8C_4C_3) - (\delta\ O_9C_4C_3)$	$(\delta\ O_8C_4C_3) - (\delta\ O_9C_4C_3)$
S18	B_u	δ CC=C a.	δ CC=C	$2(\delta\ C_1C_2C_3) - (\delta\ C_1C_2H_{12}) - (\delta\ C_3C_2H_{12}) - 2(\delta\ C_4C_3C_2) + (\delta\ C_4C_3H_{11}) + (\delta\ C_2C_3H_{11})$	$2(\delta\ C_1C_2C_3) - (\delta\ C_1C_2H_{12}) - (\delta\ C_3C_2H_{12})$
S19	A_g	δ CC=C	δ CC=C′	$2(\delta\ C_1C_2C_3) - (\delta\ C_1C_2H_{12}) - (\delta\ C_3C_2H_{12}) + 2(\delta\ C_4C_3C_2) - (\delta\ C_4C_3H_{11}) - (\delta\ C_2C_3H_{11})$	$2(\delta\ C_4C_3C_2) - (\delta\ C_4C_3H_{11}) - (\delta\ C_2C_3H_{11})$
S20	B_u	δ CCH a.	δ CCH	$(\delta\ C_1C_2C_3) - (\delta\ C_3C_2H_{12}) - (\delta\ C_4C_3C_2) + (\delta\ C_2C_3H_{11})$	$(\delta\ C_1C_2C_3) - (\delta\ C_3C_2H_{12})$
S21	A_g	δ CCH	δ CCH′	$(\delta\ C_1C_2C_3) - (\delta\ C_3C_2H_{12}) + (\delta\ C_4C_3C_2) - (\delta\ C_2C_3H_{11})$	$(\delta\ C_4C_3C_2) - (\delta\ C_2C_3H_{11})$
S22	B_g	γ C=O a.	γ C=O	$(\gamma\ C_1{=}O_5) - (\gamma\ C_4{=}O_8)$	$\gamma\ C_1{=}O_5$
S23	A_u	γ C=O	γ C=O′	$(\gamma\ C_1{=}O_5) + (\gamma\ C_4{=}O_8)$	$\gamma\ C_4{=}O_8$
S24	B_g	γ CH a.	γ CH	$(\gamma\ C_2H_{12}) - (\gamma\ C_3H_{11})$	$\gamma\ C_2H_{12}$
S25	A_u	γ CH	γ CH′	$(\gamma\ C_2H_{12}) + (\gamma\ C_3H_{11})$	$\gamma\ C_3H_{11}$
S26	B_g	τ C−O a.	τ C−O	$(\tau\ C_1{-}O_6) - (\tau\ C_4{-}O_9)$	$\tau\ C_1{-}O_6$
S27	A_u	τ C−O	τ C−O′	$(\tau\ C_1{-}O_6) + (\tau\ C_4{-}O_9)$	$\tau\ C_4{-}O_9$
S28	B_g	τ C−C a.	τ C−C	$(\tau\ C_1{-}C_2) - (\tau\ C_3{-}C_4)$	$\tau\ C_1{-}C_2$
S29	A_u	τ C−C	τ C−C′	$(\tau\ C_1{-}C_2) + (\tau\ C_3{-}C_4)$	$\tau\ C_3{-}C_4$
S30	A_u	τ C=C	τ C=C	$\tau\ C_2{=}C_3$	$\tau\ C_2{=}C_3$

[a] Symmetry species refer to the higher symmetry conformer (C_{2h}). [b] Used in the normal coordinate analysis of conformers I and II of maleic acid and form II of fumaric acid. [c] Used in the normal coordinate analysis of forms I and III of fumaric acid. [c] a., asymmetric; υ, stretching; δ, bending; γ, rocking; τ, torsion, ′, $O_8{=}C_4({-}O_9{-}H_{10}){-}C_3({-}H_{12})$ fragment. [d] For atom numbering see Figures 1 and 2.

and B3LYP) lead to qualitatively similar results. All methods predict three planar conformers (I, II, and III in Figure 2), which have relative energies within 5 kJ mol^{-1}and two conformers (IV and V in Figure 2) ca. 25 kJ mol^{-1} above these three planar structures. The planar conformers exhibit cis arrangements around the C−O bonds, differing in the conformation assumed by their O=C−C=C axes (see Figure 2). Conformers I and III belong to the C_{2h} symmetry point group and they are characterized by two s-cis or two s-trans O=C−C=C axes, respectively. Conformer II (C_s) has one s-cis and one s-trans O=C−C=C axis. Hence, in consonance with the previously reported relative energies of the s-cis and s-trans arrangements around the C_α−C bond in α,β-unsaturated carboxylic acids,[13−15] the relative energy of the three most stable conformers of fumaric acid increases with the number of s-trans O=C−C=C axes. This correlates with the existence of attractive interactions between the oxygen atoms of the carboxylic groups and the β-hydrogen atoms (weak CH···O hydrogen bond) that are important in determining the relative energy of the three most stable conformers.[13−15] In each of the three most stable conformers of fumaric acid, two O···β-hydrogen attractions are found, as shown in Figure 2. However, this interaction is stronger when it involves the carbonyl oxygen, as this atom shows a higher

ability to act as an H-bond acceptor than the hydroxylic oxygen atom.[28] The different strengths of the CH···O=C and CH···OH interactions may hence be used to justify the energy differences between conformers I, II, and III, since there are two C−H···O=C interactions present in conformer I but only one in conformer II and none in conformer III.

Conformers IV and V are similar to conformers I and II but have one trans carboxylic group (O=C−O−H dihedral of 180°; see Figure 2); they are ca. 25−30 kJ mol^{-1} above the global minimum, structure I. Besides the general higher intrinsic energy associated with a trans O=C−O−H axis relative to a cis O=C−O−H axis,[27] in fumaric acid a trans arrangement of this axis leads to the appearance of a steric repulsion between the hydrogen atom of the trans carboxylic group and the corresponding α-hydrogen atom. These two factors account for the high energy of conformers IV and V. Note that the conformation analogous to conformer III but having one of its carboxylic groups in the trans conformation was not found to be a minimum, whichever the level of theory considered. A similar situation was observed by changing the conformation of the second carboxylic group in structure II. This can be explained considering that, in these cases, the molecule is strongly destabilized by the presence of strong H···H repulsive

TABLE 4: Observed (Ar matrix) and Calculated B3LYP/6-31G(d,p) Vibrational Frequencies and IR Intensities[a] of the Most Stable Conformer of Maleic Acid

	Bands Increasing in Intensity upon NIR Irradiation and Annealing of the Matrix Assigned to Conformer I				
approximate description	ν_{exp}[b]	I_{exp}	ν_{calc}	I_{calc}	PED[c]
ν OH′	3550	29	3610	22	ν OH′ (100)
ν OH	3110	52	3210	137	ν OH (100)
ν CH	n.o.		3088	<1	ν CH (55) + ν CH′ (44)
ν CH′	n.o.		3072	<1	ν CH′ (54) + ν CH (44)
	2784	9			2 × 1410[d]
	2770	4			2 × 1403[d]
ν C=O	1762	15	1754	44	ν C=O (63)
	1750	21			
	1740	4			
ν C=O′	1722	35	1699	67	ν C=O′ (62)
	1712	9			2 × 857[d]
ν C=C	1635	26	1629	20	ν C=C (66)
	1568	6			1202 + 374[d]
δ COH	1428	36	1405	46	δ COH (68)
	1420	47			
δ CCH′	1410	13	1396	27	δ CCH′ (26)
	1406	7			
	1403	43			
	1369	4			606 + 767[d]
δ COH′	1313	8	1296	6	δ COH′ (23) + δ CCH (22)
ν C−O	1296	2	1276	2	ν C−O (32)
	1246	13			2 × 631[d]
δ CCH	1202	8		8	589 + 606[d]
	1174	26	1187		δ CCH (17) + δ CCH′ (23) + ν C−O (17)
ν C−O′	**1154**	7	1147	82	ν C−O′ (35) + δ COH′ (36)
	1152	66			
	1138	7			589 + 552[d]
γ CH	1025	2	993	<1	γ CH (53) + γ CH′ (32) + τ C=C (23)
	1027	<1			
ν C−C′	933	<1	915	4	ν C−C′ (19) + δ CCC′ (32) + δ CCC (23)
γ CH′	857	15	830	8	γ CH′ (41) + γ CH (24)
τ C−O	822	35	789	23	τ C−O (46) + τ C=C (18)
ν C−O	782	3	806	<1	ν C−C (26) + δ OCO (19)
δ CCC	775	3	746	2	δ CCC (31) + δ CCC′ (27)
γ C=O′	767	3	737	2	γ C=O′ (18) + τ C=C (29)
τ C−O′	**631**	34	640	25	τ C−O′ (57) + τ C=C (17)
δ OCO′	606	16	584	7	δ OCO′ (26) + δ OCO (20) + δ CCC (14)
δ OCO	589	19	568	9	δ OCO (33) + δ OCO′ (29)
γ C=O	552	3	544	3	γ C=O (23) + γ C=O′ (24) + γ CH (17)
δ CC=O			374	<1	δ CC=O (38) + δ CC=O′ (27)
δ CC=O′			280	2	δ CC=O′ (15) + δ CCC (38) + δ CCC′ (22)
τ C=C			271	2	τ C=C (60) + τ C−C (18)
δ CCC′			234	1	δ CCC′ (59)
τ C−C′			88	<1	τ C−C′ (48) + τ C−C (45)
τ C−C			46	<1	τ C−C (63)

[a] Frequencies in cm^{-1}; intensities in km mol^{-1}; calculated frequencies were scaled by 0.9614; experimental intensity values presented correspond to the observed integrated intensities of each conformer normalized to 1000. Calculated intensities were scaled to experimental integrated normalized intensities (only bands which have an experimental counterpart and can be ascribable to a single conformer were used in the scaling procedure). [b] Frequency values shown in bold represent bands assigned to more than one conformer. In these case, the experimental intensities shall be compared with the sum of the calculated intensities for the two observed conformers (see also Table 5). [c] Only contributions higher than 15% are listed. [d] Tentative assignment as nonfundamental modes (overtones and combination bands). ν, stretching; δ, bending; τ, torsion; γ, rocking, n.o., non observed; ′, refers to O$_8$=C$_4$(−O$_9$−H$_{10}$)−C$_3$(−H$_{12}$) fragment. Minor bands due to nonfundamental modes where also observed at 2686, 1573, 1567, 1540, 1537, and 1454 cm^{-1}.

interactions between the hydrogen atom of the trans carboxylic group and the β-hydrogen atom. On the other hand, the conformation analogous to conformer I with both carboxylic groups trans, was predicted to have an energy that is nearly twice that calculated for the structure showing only one trans carboxylic group (this conformation was predicted to be a minimum on the B3LYP PES, while it was found to correspond to a saddle point on the MP2 PES).

In Table 2 we present the geometrical parameters of the three most stable conformers of fumaric acid. In agreement with our previous studies on α,β-unsaturated carboxylic acids,[13,15] the present calculations show that a s-trans O=C−C=C axis favors the π electron delocalization in the molecule. This effect reflects

the dependence of the C$_\alpha$−C and C=C bond lengths on the conformation of the O=C−C=C axis. The C$_\alpha$−C bond length decreases and the C=C bond elongates slightly for a s-trans conformation compared to the situation in conformer I. For instance, the C$_\alpha$−C and C=C bond lengths are predicted by the MP2 calculations to be 147.9 and 134.3 pm, respectively, in conformer III, while in the most stable conformer these bond lengths are 148.2 and 134.2 pm.

Matrix-Isolation Infrared Studies. The infrared spectrum of isolated maleic and fumaric acid in solid argon clearly reveals the presence several conformers. A detailed assignment of the spectra was undertaken by comparison with previous studies of other α,β-unsaturated carboxylic acids[13−15] and with the

Study of Fumaricand Maleic Acid

J. Phys. Chem. A, Vol. 105, No. 15, 2001 **3927**

TABLE 5: Observed (Ar matrix) and Calculated B3LYP/6-31G(d,p) Vibrational Frequencies and IR Intensities[a] of Conformer II of Maleic Acid

Bands Decreasing in Intensity upon NIR Irradiation and Annealing of the Matrix Assigned to Conformer II					
approximate description	$\nu_{exp}{}^b$	I_{exp}	ν_{calc}	I_{calc}	PED[c]
ν OH′	3566	6	3616	14	ν OH′ (100)
ν OH	3561	11	3600	13	ν OH (100)
ν CH′	n.o.		3091	<1	ν CH′ (88)
ν CH	n.o.		3066	<1	ν CH (88)
ν C=O	1808	1	1772	53	ν C=O (78)
	1780	5			
	1796	1			
	1790	5			
	1783	4			
	1778	11			
	1773	13			
	1769	9			
ν C=O′	1761	13	1756	45	ν C=O′ (77)
	1754	4			
ν C=C	1698	6	1649	12	ν C=C (71)
	1570	<1			1122 + 448[d]
δ CCH′	**1420**	47	1394	47	δ CCH′ (29) + δ CCH (17)
ν C−O	1370	7	1328	8	ν C−O (23) + δ COH (22)
δ COH′	1290	3	1279	3	δ COH′ (29) + δ CCH (24)
δ CCH	1163	4	1179	9	δ CCH (39) + δ CCH′ (26)
δ COH	1150	33	1148	44	δ COH (29) + ν C−O (24)
	1147	8			
ν C−O′	1122	66	1114	77	ν C−O′ (30) + δ COH′ (21)
γ CH′	n.o.		958	<1	γ CH′ (49) + γ CH (38)
ν C−C′	934	7	926	1	ν C−C′ (21) + δ CCC′ (19) + δ CCC (19)
ν C−C	828	5	809	3	ν C−C (20) + ν C−C′ (25)
γ C=O′	811	11	792	10	γ C=O′ (29) + γ CH′ (31) + γ C=O (17)
γ C=O	781	3	762	7	γ C=O (26)
γCH	n.o.		718	3	γ CH (23) + τ C=C (21) + γ C=O′ (19)
τ C−O	**631**	34	645	10	τ C−O (44)
τ C−O′	591	8	607	13	τ C−O′ (54) + τ C=C (23)
δ OCO′	568	13	567	20	δ OCO′ (33) + τ C−O (30)
δ OCO	549	23	532	13	δ OCO (59))
δ CCC′	n.o.		451	2	δ CCC′ (15) + γ C=O (24) + δ OCO′ (19)
δ CC=O	n.o.		425	3	δ CC=O (24) + τ C=C (27) + γ CH′ (24)
δ CC=O′			272	<1	δ CC=O′ (34) + δ CCC (20)
τ C=C			224	<1	τ C=C (58)
δ CCC			135	<1	δ CCC (43) + δ CCC′ (33)
τ C−C′			78	<1	τ C−C′ (26) + τ C−C (17) + δ CCC′ (17)
τ C−C			33	<1	τ C−C (64)

[a] Frequencies in cm^{-1}; intensities in km mol^{-1}; calculated frequencies were scaled by 0.9614; experimental intensity values presented correspond to the observed integrated intensities of each conformer normalized to 1000. Calculated intensities were scaled to experimental integrated normalized intensities (only bands which have an experimental counterpart and can be ascribable to a single conformer were used in the scaling procedure). [b] Frequency values shown in bold represent bands assigned to more than one conformer. In these case, the experimental intensities shall be compared with the sum of the calculated intensities for the two observed conformers (see also Table 4). [c] Only contributions higher than 15% are listed. [d] Tentative assignment as combination band. υ, stretching; δ, bending; τ, torsion; γ, rocking, n.o., non observed; ′, refers to $O_8=C_4(-O_9-H_{10})-C_3(-H_{12})$ fragment. Minor bands due to nonfundamental modes where also observed at 2686, 1568, 1539, 1343, 1341, and 1186 cm^{-1}.

calculated spectra (B3LYP). Besides, results from annealing experiments and in situ near-infrared (NIR) irradiation of the matrix sample showing conformational isomerization of the studied molecules were also used to assign the experimentally observed absorptions.

Table 3 presents the symmetry coordinates used to perform the normal coordinate analysis. We have used two different sets of symmetry coordinates, one for the conformers of maleic and fumaric acid belonging either to the C_s or C_1 symmetry point groups and another for the C_{2h} conformers of fumaric acid.

Maleic Acid. The experimental and calculated wavenumbers and intensities as well as potential energy distribution (PED) for the observed absorption bands of maleic acid are collected in Tables 4 and 5. For maleic acid we were able to promote conformer isomerization both by NIR irradiation and annealing of the matrix. Therefore, the assignment of the bands of the various conformers of maleic acid is rather straightforward: the increasing bands upon NIR irradiation and annealing at 35 K

are ascribable to the lowest energy conformer (conformer I) and the decreasing bands belong to the second most stable conformer predicted by the calculations (conformer II). No evidence was found of presence of other conformers.

The IR spectrum of matrix isolated maleic acid is shown in Figure 3. In the OH stretching region, the spectrum shows bands at 3566, 3560, and 3550 cm^{-1}, which are typical values for an O−H group not involved in hydrogen bonding (see Figure 3a). The intense band at ∼3110 cm^{-1}, can be assigned to an O−H group participating in a strong hydrogen bond. According to the calculations, we assign the higher frequency bands to conformer II. The bands at 3550 and 3110 cm^{-1} are due to the vibrations of the free and intramolecularly hydrogen bonded OH group of the most stable conformer, respectively.

In the C=O stretching region, a complex multiplet of bands appears in the 1808−1754 cm^{-1} region, which are due to carbonyl groups not involved in hydrogen bonding. Besides this multiplet, an intense carbonyl band is found at 1722 cm^{-1}, and
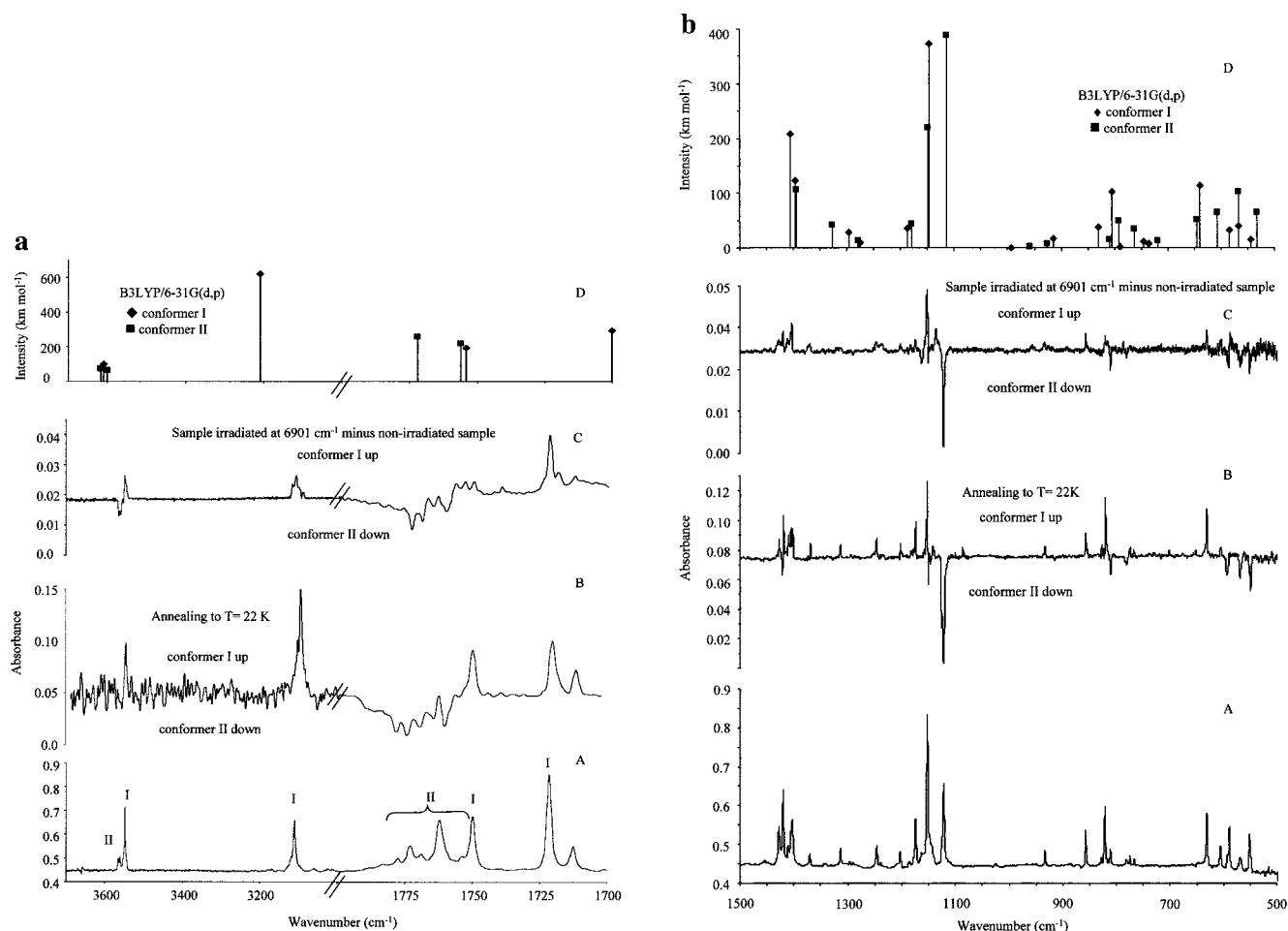
Figure 3. IR spectra of maleic acid [(a) 3600−3000 cm⁻¹ region, (b) 1500−500 cm⁻¹ region], (A) Ar matrix (*T* = 7.5 K); (B) difference spectrum (spectrum at *T* = 22 K minus spectrum at *T* = 9 K); (C) difference spectrum (irradiated matrix at 6901 cm⁻¹ minus nonirradiated sample); (D) calculated spectra (B3LYP).

it is red shifted (due to hydrogen bonding) compared with the unperturbed carbonyl absorptions. Taking into consideration the theoretical results, the latter band is assigned to the C=O stretching mode of the hydrogen bonded carbonyl of conformer I, while the different components are ascribed to the vibrations originated from the non-hydrogen-bonded carbonyl of conformers I and II.

As shown in Figure 3b, the results obtained for other spectral regions fully agree with the discussion above made for the OH and C=O stretching regions. For example, the most intense band in the spectrum, which appears as a doublet at 1154 and 1152 cm⁻¹ is ascribed to the ν C−O′ mode in conformer I that is predicted by the calculations at 1148 cm⁻¹. In the difference spectra showing the results of irradiation and annealing (B and C in Figure 3b) it is clear that, overlapped with the 1152 cm⁻¹ band, a doublet appears with frequency maxima at 1150 and 1147 cm⁻¹ which is due to conformer II and is assigned to δ COH of this form (calculated value, 1148 cm⁻¹). The ν C−O′ mode in conformer II is predicted at 1114 cm⁻¹ and is easily assigned to the band at 1122 cm⁻¹ that decreases in intensity upon irradiation and after annealing. In turn, δ COH in conformer I (calculated value: 1405 cm⁻¹) gives rise to a doublet at 1428 and 1420 cm⁻¹ (the low-frequency component is superimposed with the δ CCH′ mode of conformer II—calculated value, 1394 cm⁻¹—as noticed in the difference spectra).

The bands ascribed to ν C−O and δ COH′ are considerably less intense (see Tables 4 and 5) than those due to ν C−O′ and

δ COH but, nevertheless, their assignment was not difficult since they lie in less congested spectral regions.

The bands associated with vibrations involving mainly bonds with large dipole moments, such as the C=O and C−O stretching modes and the COH bendings, appear site-splitted in the matrix experiments. This fact is particularly evident for the vibrations of conformer II, where 10 component bands are ascribable to the C=O stretching modes.

Fumaric Acid. The assignment of the infrared spectrum of fumaric acid is presented in Tables 6 and 7. For this molecule, the assignments were made basically taking into consideration the calculated spectra for the three most stable conformers, since either annealing or irradiation (both narrowband tunable NIR and broadband IR irradiation) of the matrix did not lead to any observable changes in the spectrum. Thus, the proposed assignments for fumaric acid have a higher uncertainty than those presented for maleic acid, especially for bands appearing in more congested spectral regions. Moreover, the structure of the three low-energy conformers of fumaric acid is relatively similar (e.g., all carboxylic groups are in the cis conformation), leading to similar frequencies for the various conformers hence making their detailed assignment more difficult.

The presence of conformer II in the matrix is unequivocal, since this is a conformer of fumaric acid that has no symmetry restrictions for observation of any fundamental vibrations. Thus, for instance, the band observed at 1650 cm⁻¹, which is a characteristic absorption band of a C=C stretching mode, should be assigned to this conformer, since this vibration (A_g) is IR-

Study of Fumaricand Maleic Acid

J. Phys. Chem. A, Vol. 105, No. 15, 2001 **3929**

TABLE 6: Observed (Ar matrix) and Calculated B3LYP/6-31G(d,p) Vibrational Frequencies and IR Intensities[a] of Conformers I and III of Fumaric Acid (C_{2h} Symmetry)

approximate description	conformer I					conformer III				
	ν_{exp}[b]	I_{exp}	ν_{calc}	I_{calc}	PED[c]	ν_{exp}[b]	I_{exp}	ν_{calc}	I_{calc}	PED[c]
ν O—H a.	**3560**	54	3611	31	ν O—H a. (100)	**3576**	22	3620	19	ν O—H a. (100)
ν CH a.	**2948**	27	3099	<1	ν CH a. (100)	**2948**	27	3113	<1	ν CH a. (100)
ν C=O a.	**1765**	16	1750	97	ν C=O a. (78)	**1765**	16	1754	74	ν C=O a. (79)
	1763	15				**1763**	15			
	1759	29				**1759**	29			
	1756	84				**1756**	84			
	1754	38				**1754**	38			
	1750	39				**1750**	39			
						1388	4			1256 + 133[d]
ν C—O a.	1369	61	1352	71	ν C—O a. (27) + δ COH a. (27) + ν C—C a. (22)	1315	15	1331	21	ν C—O a. (25) + ν C—C a. (23)
						1311	13			
δ CCH a.	1217	11	1207	43	δ CCH a. (83)	1256	30	1222	4	δ CCH a. (47) + δ COH a. (40)
	1211	7								
δ COH a.	1115	46	1103	101	δ COH a. (43) + ν C—O a. (28)	1132	52	1128	63	δ COH a. (22) + ν C—O a. (39) + δ CCH a. (29)
	1111	10								
γ CH	982	8	988	6	γ CH (99)	988	9	995	4	γ CH (99)
ν C—C a.	914	2	891	1	ν C—C a. (59) + ν C—O a. (23)	902	1	883	1	ν C—C a. (66) + ν C—O a. (24)
γ C=O	**777**	31	757	19	γ C=O (59) + τ C—O (21)	**777**	31	757	9	γ C=O (52) + τ C—O (26)
δ OCO a.	600	8	614	41	δ OCO a. (68)	560	6	577	17	δ OCO a. (65)
	599	30				557	4	577	19	τ C—O (80)
τ C—O	571	44	581	20	τ C—O (87)					
δ CC=O a.	**537**	7	520	10	δ CC=O a. (55) + δ CCC a. (17) + δ OCO a. (16)	**537**	7	520	4	δ CC=O a. (53) + δ OCO a. (19)
τ C=C			141	<1	τ C=C (60) + γ CH (30)			137	<1	τ C=C (62) + γ CH (31)
δ CCC a.			122	<1	δ CCC a. (77) + δ CC=O a. (21)			133	<1	δ CCC a. (75) + δ CC=O a. (22)
τ C—C			52	<1	τ C—C (61) + γ CH (22)			48	<1	τ C—C (88)

[a] Frequencies in cm^{-1}; intensities in km mol^{-1}; calculated frequencies were scaled by 0.9614; experimental intensity values presented correspond to the observed integrated intensities of each conformer normalized to 1000. Calculated intensities were scaled to experimental integrated normalized intensities (only bands which have an experimental counterpart and can be ascribable to a single conformer were used in the scaling procedure). [b] Frequency values shown in bold represent bands assigned to more than one conformer. In these case, the experimental intensities shall be compared with the sum of the calculated intensities for the three observed conformers (see also Table 7). [c] Only contributions higher than 15% are listed. [d] Tentative assignment as combination band. υ, stretching; δ, bending; τ, torsion; γ, rocking. Minor bands due to nonfundamental modes are also observed at 1808, 1794, 1348, 1320, 1301, 1190, 1106, 714, 712 cm^{-1}.

inactive in conformers I and III belonging to the C_{2h} symmetry point group. The presence of conformers I and III in the matrix can also be clearly established as described below. It is interesting to note that a recent study on matrix isolated fumaryl chloride [(E)-ClC(=O)—C=C—(C=O)Cl] succeeded to observe the three conformers of that molecule which are the analogous chlorine-substituted forms of the three most stable conformers of fumaric acid predicted by the calculations.[29]

In the OH stretching region, the band observed at the highest wavenumber (3576 cm^{-1}) is assigned to conformers II and III, both having bands predicted to occur at 3620 cm^{-1} (Figure 4a). The two bands at lower wavenumbers (~3560 cm^{-1}) are assigned to the asymmetric OH stretching mode of conformer I and to the second OH stretching vibration of conformer II. Both vibrational modes are computed to lie at ca. 3610 cm^{-1}. The broad band observed at 2948 cm^{-1} is attributed to the IR active stretching C—H vibrations of the three conformers, predicted to lie in the 3115—3050 cm^{-1} region and being very weak.

As expected, taking into consideration the structural similarity of the three experimentally observed conformers of fumaric acid, their C=O stretching modes appear as a "complex band" with six components separated by a few wavenumbers in the 1765 to 1750 cm^{-1} region. Although it was not possible to make a detailed assignment of this multiplet, the calculations indicate that its higher wavenumber components should be mainly due to the C=O stretching mode of conformer II, which is predicted to occur at 1760 cm^{-1}. The lower wavenumber components is suitable to the second vibration of this conformer (predicted at 1753 cm^{-1}) as well as to the C=O asymmetric stretching modes

of conformers I and III (that are predicted at 1750 and 1754 cm^{-1}, respectively).

The strongest support for the presence of three conformers of fumaric acid in the matrix can be found in the C—O stretching region. The C—O stretching in conformer I is predicted to occur at higher frequency (1352 cm^{-1}) than for conformer III (1331 cm^{-1}), while the two C—O vibrations of conformer II are predicted to occupy intermediate wavenumbers (1345 and 1337 cm^{-1}). The experimental spectrum exhibits the same pattern in this spectral region (Figure 4b; see also Tables 6 and 7). The band observed at 1369 cm^{-1} is ascribable to the C—O stretching mode of conformer I. The two C—O stretching modes of conformer II give rise to the band at 1338 cm^{-1} and the doublet at 1364 and 1357 cm^{-1} (in the last case, the observed splitting results from matrix site effects). The lowest site-splitted band found at 1315 and 1311 cm^{-1} is due to conformer III.

The agreement between the predicted and experimental spectra is also quite clear in the in-plane COH bending region (Figure 4b), where the bands belonging to conformer II (predicted at 1154 and 1116 cm^{-1}) are observed at 1158 and 1120 cm^{-1}. The vibrational modes of conformers I and III (predicted at 1103 and 1128 cm^{-1}, respectively) are observed at 1115—1111 cm^{-1}and 1132 cm^{-1}.

NIR Irradiation and Annealing Experiments. Selective irradiation of the OH stretching vibrations have been demonstrated to be a very elegant way of promoting conformational isomerization processes in matrix isolated carboxylic compounds.[24–26,30] The use of narrow band tunable irradiation in the NIR region, at a frequency of the first OH stretching overtone or a suitable combination was found to be particularly

TABLE 7: Observed (Ar matrix) and Calculated B3LYP/6-31G(d,p) Vibrational Frequencies and IR Intensities[a] of Conformer II of Fumaric Acid (C_S Symmetry)

aproximate description	ν_{exp}	I_{exp}	ν_{calc}	I_{calc}	PED[b]
ν O–H	**3576**	22	3620	14	ν O–H (100)
ν O–H′	**3560**	27	3610	14	ν O–H′ (100)
ν CH′	2948	27	3106	<1	ν CH′ (89)
ν CH			3101		ν CH (88)
ν C=O	**1765**	16	1760	19	ν C=O (47) + ν C=O′ (26)
	1763	15	1753	67	ν C=O′ (51) + ν C=O (28)
	1759	29			
	1756	84			
ν C=O′	**1754**	38			
	1750	39			
ν C=C	1650	18	1651	6	ν C=C (66)
ν C–O′	1364	35	1345	33	ν C–O′ (18)
	1357	8			
ν C–O	1338	9	1337	10	ν C–O (23) + δ COH (16)
δ CCH	1274	3	1257	<1	δ CCH (40) + δ CCH′ (24)
	1269	<1			
	1242	2			986 + 257[d]
δ CCH′	1234	14	1213	12	δ CCH′ (26) + δ CCH (36) + δ COH′ (21)
δ COH	1158	17	1154	48	δ COH (46) + ν C–O (21)
δ COH′	1120	52	1116	50	δ COH′ (24) + ν C–O′ (38) + δ CCH′ (16)
γ CH	986	11	994	6	γ CH (65) + γ CH′ (34)
ν C–C′	938	4	917	3	ν C–C′ (48)
γ CH′	909	2	885	<1	γ CH′ (46) + γ CH (36)
ν C–C	896	2	879	<1	ν C–C (41) + ν C–O (36)
γ C=O′	**777**	31	757	14	γ C=O′ (30) + γ C=O (26)
τ C–O′	n. o.		667	2	τ C–O′ (29) + τ C–O (19) + γ C=O (19)
δ OCO′	n. o.		640	<1	δ OCO′ (35) + δ OCO (24)
τ C–O	589	50	592	34	τ C–O (58) + τ C–O′ (23)
δ OCO	554	10	568	17	δ OCO (51) + δ OCO′ (31)
γ C=O	546	3	544	<1	γ C=O (29) + γ C=O′ (24)
δ CC=O			529	3	δ CC=O (38) + δ CC=O′ (28)
δ CC=O′			371	<1	δ CC=O′ (30) + δ CC=O (24)
δ CCC′			257	<1	δ CCC′ (24) + δ CCC (20)
τ C=C			141	<1	τ C=C (65) + γ CH (16)
τ C–C′			138	<1	τ C–C′ (41) + τ C–C (37)
δ CCC			128	<1	δ CCC (38) + δ CCC′ (38)
τ C–C			50	<1	τ C–C (50) + τ C–C′ (27)

[a] Frequencies in cm^{-1}; intensities in km mol^{-1}; calculated frequencies were scaled by 0.9614; experimental intensity values presented correspond to the observed integrated intensities of each conformer normalized to 1000. Calculated intensities were scaled to experimental integrated normalized intensities (only bands which have an experimental counterpart and can be ascribable to a single conformer were used in the scaling procedure). [b] Frequency values shown in bold represent bands assigned to more than one conformer. In these case, the experimental intensities shall be compared with the sum of the calculated intensities for the three observed conformers (see also Table 6). [c] Only contributions higher than 15% are listed. v, stretching; δ, bending; τ, torsion; γ, rocking, ′, refers to O$_8$=C$_4$(–O$_9$–H$_{10}$)-C$_3$(–H$_{12}$) fragment. Minor bands due to nonfundamental modes are also observed at 1808, 1794, 1348, 1320, 1301, 1190, 1106, 714, 712 cm^{-1}.

efficient in initiating the conformational isomerization of matrix-isolated oxalic and malonic acids.[22,25] In the present study NIR irradiation of matrix-isolated maleic and fumaric acids, in the 7020–6830 cm^{-1} region, was undertaken.

For maleic acid, the irradiation experiments unequivocally confirmed the computational results with respect to the most stable conformers. Irradiation of the matrix at 6901 cm^{-1} led to an increase of the bands assigned to conformer I, while bands due to conformer II decreased (see Figure 3), which indicates that the NIR-irradiation is effective in promoting interconversion from conformer II to the most stable conformer I.

In the case of fumaric acid, irradiation all over the region covered (7018–6873 cm^{-1}) was found to be inefficient to initiate any conformational isomerization process. Note that the first overtone of the OH stretching mode in fumaric acid is expected to lie in the 6996–6940 cm^{-1} region, taking into account the results of previous studies undertaken on malonic acid.[22] In fact, it has been shown that in this kind of molecules anharmonicity associated with the OH stretching vibration may

account for a red shift of ca. 160 cm^{-1} in the position of its first overtone when compared with twice the fundamental frequency.

The observed inefficiency of irradiation at the first overtone of the OH stretching mode in fumaric acid to promote interconversion between the low-energy observed conformers may have the same origin as the previously reported failure to promote by this way isomerization reactions implying internal rotation around the C–C central bond in oxalic acid.[25] This was explained on the basis of the extensive matrix reorganization required by internal rotation about the C–C bond, which involves a relatively large motion of the molecular fragments. This rearrangement leads to considerably higher effective energy barriers when compared with the molecule in the vacuum.[25] Further support to this interpretation can also be taken from recent studies on matrix isolated oxalyl fluoride and nitrous acid,[31,32] which clearly demonstrated that isomerization processes induced by narrowband IR radiation can be selective with respect to the matrix sites, and no significant matrix rearrangements occur. Note that in maleic acid the observed intercon-
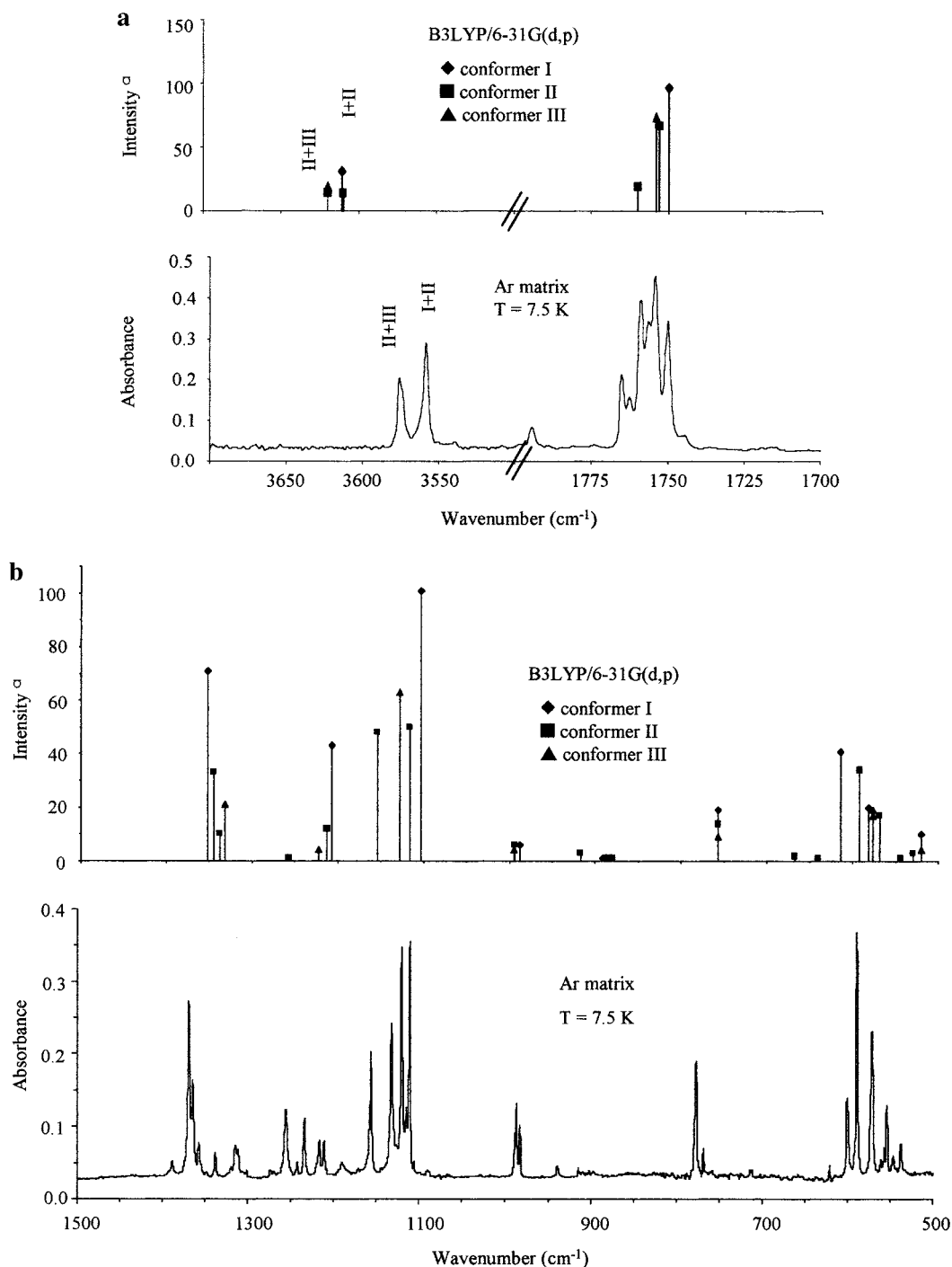
Study of Fumaricand Maleic Acid

J. Phys. Chem. A, Vol. 105, No. 15, 2001 **3931**

Figure 4. IR spectrum of fumaric acid in an argon matrix ($T = 7.5$ K) and predicted (B3LYP) spectra for the three lowest energy conformers: (a) $3700-1700$ cm^{-1} region and (b) $1500-500$ cm^{-1} region. [a]Calculated intensities as shown in Tables 6 and 7 where the normalization procedure is explained in detail.

version processes involve only small adjustments in the positions of the heavy atoms and so, contrary to the rotamerization processes in fumaric acid, these processes do not require any significant matrix rearrangements.

The lack of NIR induced isomerization processes in fumaric acid might also be attributed to the absence of any suitable mechanism for energy transfer between the excited vibrational mode and the reaction coordinates (ν OH overtone and the τ C−C, respectively) or weak absorption by the overtone. Nevertheless, the fact that broadband IR irradiation was also unable to promote any observable isomerization process in fumaric acid seems to indicate that, as discussed above, relatively high energy barriers for conformational isomerization

in fumaric acid (associated in some extent with matrix relaxation) shall, at least in part, explain the different behavior of the two studied compounds.

UV irradiation ($\lambda = 266$ nm) of fumaric acid in argon matrixes was also performed. As shown in Figure 5, UV excitation efficiently promotes isomerization of fumaric acid to maleic acid. On the other hand, no detectable conformational interconversion between the observed conformers of fumaric acid could be observed. A similar photochemically induced tautomerization reaction was also previously observed for matrix isolated fumaryl chloride ($\lambda = 340$ nm).[29] In this case, maleoyl chloride was produced, and, as for fumaric acid, no conforma-
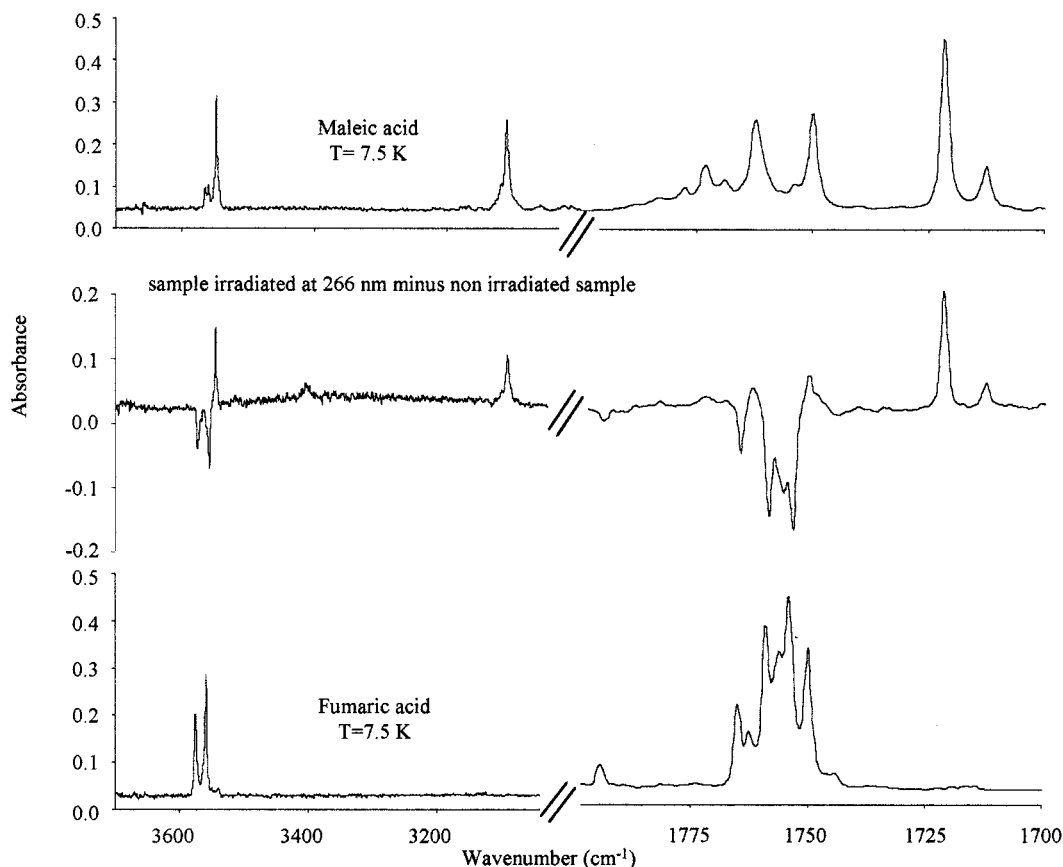
Figure 5. Matrix isolation IR spectra of maleic (top) and fumaric (bottom) acids and difference spectra obtained by subtracting to the spectrum of a freshly prepared matrix of fumaric acid from the spectrum of the same sample after UV irradiation at 266 nm (middle).

tional interconversion between the conformers initially present in the matrix could be observed.

We have also studied the thermally induced conformational isomerization for maleic and fumaric acids by annealing freshly prepared matrixes up till 35 K. In the case of maleic acid, a noticeable redistribution of intensities starts at 22 K, clearly evidencing an increase of the relative population of the conformational ground state (Figure 3). Taking into consideration the relationship first derived by Barnes,[33] these results point to an energy barrier for conversion of conformer II into conformer I of ca. 6 kJ mol^{-1}. For fumaric acid, no changes in the spectrum attributed to rotamerization processes were observed within the experimentally accessible temperature range. This result is an additional support for the interpretation based on energy considerations, above made, to explain the absence of any photoisomerization reaction in fumaric acid. In addition, it also indicates that the energy barriers for conformer interconversion in this molecule are higher than 12 kJ mol^{-1}, the largest accessible barrier at the maximum temperature attained.[33] The MP2 calculated energy barriers associated with the studied conformational isomerization processes for fumaric acid in a vacuum amount to ca. 20 kJ mol^{-1}.

Experimental vs Calculated Populations of the Observed Conformers. Relative energies of the observed conformers can be calculated from their relative populations at a given temperature assuming a Boltzmann distribution. The relative populations of the observed conformers can be estimated from the experimental IR band intensities recorded immediately after deposition taking into account the calculated intensities and assuming that no conformational isomerization takes place during the deposition process. For maleic acid the O—H and C=O stretching regions were used in these estimations due to

the intense signals observed, as well as because these regions are not congested and can unequivocally be used to assign the different conformers. For fumaric acid, the C—O stretching, in-plane COH bending and C=O rocking spectral regions were used by the same reasons.

The energy difference between the two observed conformers of maleic acid obtained by this method is 1.7 kJ mol^{-1}, which is in excellent agreement with the MP2 predictions (1.3 kJ mol^{-1}). For fumaric acid, a good qualitative agreement between the ab initio and the experimentally determined relative energies of the conformers was also obtained, although the theoretical predictions at all levels used systematically give higher values (measured, $E_{II} - E_I = 0.7$ kJ mol^{-1} and $E_{III} - E_I = 0.9$ kJ mol^{-1}; MP2, $E_{II} - E_I = 2.3$ kJ mol^{-1} and $E_{III} - E_I = 4.6$ kJ mol^{-1}).

Conclusion

The ab initio calculations carried out at the MP2 and B3LYP levels were used to characterize the most stable conformers of maleic and fumaric acids and the computational results were used to aid the interpretation of the infrared spectra of these compounds isolated in an argon matrix. The lowest energy conformer of maleic acid was found to exhibit a nearly planar structure with an OH···O=C intramolecular hydrogen bond closing a seven member O=C—C(H)=C(H)—C—O—H ring. The second conformer of maleic acid adopts a cis arrangement around the C—O bonds and exhibits two carbonyl bonds in a nearly orthogonal arrangement with one carboxylic group in the plane containing the carbon atoms. For fumaric acid, three low-energy conformers exhibiting a cis arrangement around the C—O bond where found computationally and experimentally.

The conformers differ by the relative conformation of their O=C−C=C axes and were predicted to be almost equal energetically.

The use of narrow band tunable NIR irradiation at the first OH stretching overtone together with the annealing of the matrix up to 35 K allowed us to directly observe conformational isomerization between the low-energy conformers of matrix-isolated maleic acid. On the other hand, no conformational interconversions were observed for fumaric acid by vibrational excitation (both in the NIR and mid-IR regions) or annealing. This points to relatively high energy barriers to internal rotation in matrix-isolated fumaric acid. A lower limit of ca. 12 k J mol^{-1}, resulting from the annealing studies, can be estimated for these barriers in fumaric acid, this value being nearly twice the energy barrier associated with the observed rotamerization processes in maleic acid.

References and Notes

(1) Muller. *Corros. Sci.* **1995**, *37*, 877.

(2) Solich, M.; Krol, W.; Skirmuntt, K. *Pol. J. Chem.* **1993**, *67*, 433.

(3) Kawaguchi, S.; Kitano, T.; Ito, K. *Macromolecules* **1992**, *25*, 1294.

(4) Wang, F. C.; Green, J. G.; Gerhart, B. B. *Anal. Chem.* **1996**, *68*, 2477.

(5) Eiem-Ong, S.; Spohn, M.; Kurtzman, N. A.; Sabatini, S. *Kidney Int.* **1995**, *48*, 1542.

(6) Castrano, E. *Clin. Sci.* **1997**, *92*, 247.

(7) a) Tsuchiya, K.; Uchida, T.; Kobayashi, M.; Maeda, H.; Konno, T.; Yamanaka, H. *Urology* **2000**, *55* (4), 495. (b) Abe, S.; Okubo, Y.; Ejiri, Y.; Kume, K; Otsuki, M. *J. Gastroenterol.* **2000**, *35* (1), 28.

(8) Haan, P.; Blomberg-van der Flier, B. M. E, Groot, J.; Nieboer, C; Bruynzeel, D. P. *Dermatology* **1994**, *188*, 126.

(9) Akao, M.; Kuroda, K. *Chem. Pharm. Bull.* **1990**, *38*, 2012.

(10) Shahat, M. *Acta Crystallogr.* **1952**, *5*, 763.

(11) Brown, C. J. *Acta Crystallogr.* **1966**, *21*, 1.

(12) Bednowitz, A. L.; Post, B. *Acta Crystallogr.* **1966**, *21*, 566.

(13) Kulbida, A.; Ramos, M. N.; Räsänen, M.; Nieminen, J.; Schrems, O.; Fausto, R. *J. Chem., Soc. Faraday Trans.* **1995**, *91*, 1571.

(14) Fausto, R.; Kulbida, A.; Schrems, O. *J. Chem. Soc., Faraday Trans.* **1995**, *91*, 3755.

(15) Fausto, R.; Maçôas, E. M. S. *J. Mol. Struct.* **1999**, *480−481*, 83.

(16) Hehre, J. W.; Ditchfield, R.; Pople, J. A. *J. Chem. Phys.*, **1972**, *56*, 2257.

(17) a) Møller, C.; Plesset, M. S.; *Phys. Rev.* **1934**, *46*, 618. (b) Binkley, J. S.; Pople, J. A. *Int. J. Quantum Chem.* **1975**, *9*, 229.

(18) a) Becke, A. D. *J. Chem. Phys.* **1993**, *98*, 5648. (b) Lee, C.; Yang, W.; Parr, R. G. *Phys. Rev.* **1988**, *B37*, 785; Miehlich, B.; Savin, A.; Stoll, H.; Preuss, H.; *Chem. Phys. Lett.* **1989**, *157*, 200.

(19) a) Frisch, M. J.; Trucks, G. W.; Schlegel, H. B.; Gill, P. M. W.; Johson, B. G.; Wong, M. W.; Foresman, J. B.; Robb, M. A.; Head-Gordon, M.; Replogle, E. S.; Gomperts, R.; Andres, J. L.; Raghavachari, K.; Binkley, J. S.; Gonzalez, C.; Martin R. L.; Fox, D. J.; Defrees, D. J.; Baker, J.; Stewart, J. J. P.; Pople, J. A. GAUSSIAN92/DFT (rev. G.2), Gaussian Inc., Pittsburgh, PA, 1993. (b) Frisch, M. J.; Trucks, G. W.; Schlegel, H. B.; Gill, P. M. W.; Johson, B. G.; Robb, M. A.; Cheeseman, J. R.; Keith, T.; Petersson, G. A.; Montgomery, J. A.; Raghavachari, K.; Al-Laham, M. A.; Zakrzewski, V. G.; Ortiz, J. V.; Foresman, J. B.; Cioslowski, J.; Stefanov, B. B.; Nanayakkara, A.; Challacombe, M.; Peng, C. Y.; Ayala, P. Y.; Chen, W.; Wong, M. W.; Andres, J. L.; Replogle, E. S.; Gomperts, R.; Martin, R. L.; Fox, D. J.; Binkley, J. S.; Defrees, D. J.; Baker, J.; Stewart, J. J. P.; Head-Gordon, M.; Gonzalez, C.; Pople, J. A. GAUSSIAN 94; Gaussian Inc., Pittsburgh, PA, 1995; Revision B.1.

(20) a) Binkley, J. S.; Pople, J. A.; Hehre, W. J. *J. Am. Chem. Soc.* **1980**, *102*, 939. (b) Gordon, M. S.; Binkley, J. S.; Pople, J. A.; Pietro, W. J.; Hehre, W. J. *J. Am. Chem. Soc.* **1982**, *104*, 2797.

(21) Hariharan, P. C.; Pople, J. A. *Theor. Chim. Acta (Berl.)* **1973**, *28*, 213.

(22) Maçôas, E. M. S.; Fausto, R.; Lundell, J.; Pettersson, M.; Khriachtchev, L.; Räsänen, M, *J. Phys. Chem. A* **2000**, *104*, 11725.

(23) Fausto, R. TRANSFORMER (version 2.0); Chemistry Department, University of Coimbra, Portugal, 1997.

(24) Faria, M. D. G.; Fausto R. BUILD-G (version 2.0) and VIBRAT (version 2.0); Chemistry Department, University of Coimbra, Portugal, 1997 (these programs incorporate several routines from programs GMAT and FPERT, Fuher, H.; Kartha, V. B.; Krueger, P. J.; Mantsch, H. H. *Natl. Res. Council Can. Bull.* **1976**, *15*, 1.)

(25) Maçôas, E. M. S.; Fausto, R.; Pettersson, M.; Khriachtchev, L.; Räsänen, M. *J. Phys. Chem A* **2000**, *104*, 6956.

(26) Fausto, R. *Low-Temperature Molecular Spectroscopy*; Fausto, R., Ed.; NATO-ASI Series C483, Kluwer Academic: Amsterdam (The Netherlands), 1996; 125.

(27) Fausto, R. *Theochemistry* **1994**, *315*, 123.

(28) Batista de Carvalho, L. A. E; Teixeira-Dias, J. J. C.; Fausto, R. *Theochem.*, **1990**, 208, 109; Teixeira-Dias, J. J. C.; Batista de Carvalho, L. A. E.; Fausto, R. *J. Comput. Chem.* **1991**, *12*, 1047.

(29) Piétri, N.; Jurca, B.; Monnier, M.; Hillebrand, M.; Aycard, J. P. *Spectrochim. Acta* **1999**, *56A*, 157.

(30) Nieminen, J.; Räsänen, M.; Murto, J. *J. Phys. Chem.*, **1992**, *96*, 5303.

(31) Sander, S.; Willner, H.; Khriachtchev, L.; Pettersson, M.; Räsänen, M.; Varetti, L. *J. Mol. Spectrosc.* **2000**, *203*, 145.

(32) Khriachtchev, L.; Lundell, J.; Isoniemi, E.; Räsänen, M. *J. Chem. Phys.* **2000**, *113*, 4265.

(33) Barnes, A. J. *J. Mol. Struct.* **1984**, *113*, 161.